THE JOURNAL OF PHYSICAL CHEMISTRY B

ARTICLE

pubs.acs.org/JPCB

# Effect of Aggregation on the Photophysical Properties of Three Fluorene−Phenylene-Based Cationic Conjugated Polyelectrolytes

Matthew L. Davies,[*,†,‡,⊥] Peter Douglas,[*,†] Hugh D. Burrows,[*,‡] Maria da Graça Miguel,[‡] and Alastair Douglas[§]

[†]Chemistry Group, School of Engineering, Swansea University, Singleton Park Swansea, SA2 8PP, U.K.

[‡]Departamento de Química da Universidade de Coimbra, Rua Larga, 3004-535 Coimbra, Portugal

[§]AD Technology Consulting Limited, Swansea, SA2 7UZ, U.K.

Supporting Information

**ABSTRACT:** The effect of aggregation on the photophysical properties of three cationic poly{9,9-bis[*N*,*N*-(trimethylammonium)hexyl] fluorene-*co*-l,4-phenylene} polymers with average chain lengths of ~6, 12, and 100 repeat units (PFP-NR3$_{6(I),12(Br),100(Br)}$) has been studied by steady-state and time-resolved fluorescence techniques. Conjugated polyelectrolytes are known to aggregate in solution and for these PFP-NR3 polymers this causes a decrease in the fluorescence quantum yield. The use of acetonitrile as a cosolvent leads to the breakup of aggregates of PFP-NR3 in water; for PFP-NR3$_{6(I)}$, this results in an ~10-fold increase in fluorescence quantum yield, a ca. 2-fold increase in the molar extinction coefficient at 380 nm, and an increase in the emission lifetime, as compared with polymer behavior in water. Fluorescence anisotropy also decreases with increasing aggregation, and this is attributed to increased fluorescence depolarization by interchain energy transfer in aggregate PFP-NR3 clusters. Förster resonance energy transfer along the polymer chain is expected to be very fast, with a calculated FRET rate constant of $7.3 \times 10^{12}$ s$^{-1}$ and a Förster distance of 2.83 nm (cf. the polymer repeat unit separation of 0.840 nm) for PFP-NR3$_{100(Br)}$. The complex polymer excited-state decay kinetics in aggregated PFP-NR3 systems have been successfully modeled in terms of intrachain energy transfer via migration and trapping at interchain aggregate trap sites, with model parameters in good agreement with data from picosecond time-resolved studies and the calculated theoretical Förster energy-transfer rates.

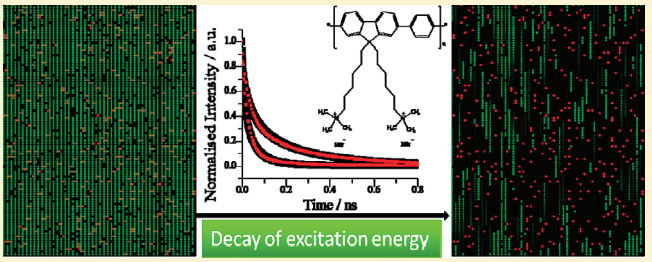


## 1. INTRODUCTION

Conjugated polyelectrolytes are currently the subject of intense research due to their exceptional optical, electronic, and mechanical properties.[1−8] Cationic conjugated polyelectrolytes (CCPs) are of particular interest. They are often highly sensitive to changes in their physical and chemical environment,[9−12] and one of the major potential uses of CCPs is in biological and chemical sensors.[3,12−14] Particular emphasis has recently focused on the use of CCPs in sequence-specific DNA assays, designed by utilizing the electrostatic interactions between CCPs and negatively charged DNA.[4,15−19] These assays commonly exploit the ability of CCPs for efficient excitation energy transfer using, for example, protein nucleic acids (PNA) and Förster resonance energy transfer (FRET).[8,19−22] Although CCPs have already been used in biosensors,[20,21] there is still a great deal of research needed to optimize their use. Two of the main areas in which a greater understanding is required are the aggregation properties and energy-transfer processes of CCPs.[9,23]

Conjugated polyelectrolytes tend to aggregate in solution due, in part, to the hydrophobicity of the backbone. This causes a decrease in emission through aggregate quenching.[10,24] Minimizing aggregation and thus maximizing emission quantum yield is important for the use of CCPs in "FRET"-type sensors, and various methods have been used to try to overcome this problem, including the incorporation of linear and branched polymer side chains and the use of surfactants.[25−31]

Exciton dynamics are also of great importance for the application of CCPs to sensors and light-emitting and photovoltaic devices.[29,30,32,33] A conjugated polymer chain can be thought of as a series of linked chromophores with a distribution of conjugation lengths that arise due to both a distribution of polymer sizes and the fact that, within a polymer, twists and bends of the chain can lead to breaks in conjugation.[33] Following light absorption, excitons are produced and move rapidly along the polymer chains. Excitation may migrate from the absorbing molecular unit over a considerable number of other units by FRET or, in some cases, by exciton hopping through Dexter transfer,[34] before deactivation occurs by fluorescence or other

**Received:** March 15, 2011
**Revised:** April 22, 2011
**Published:** May 10, 2011

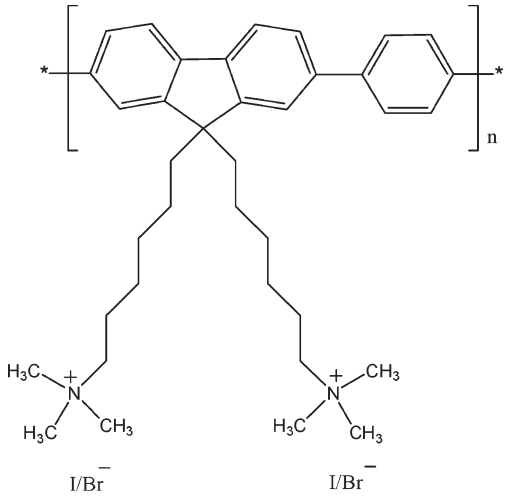


**Figure 1.** Structure of PFP-NR3.

processes.[35,36] Such energy transfer cannot be identified from fluorescence excitation or emission spectra. However, it does lead to a decrease in the fluorescence anisotropy of the system.[37,38] Exciton migration will be influenced by aggregation because this provides the possibility of both interchain FRET and the formation of aggregation "traps".

In this study, we report results from steady-state absorption, emission, fluorescence polarization, and picosecond time-resolved emission studies of the aggregation of three conjugated cationic polyelectrolytes, poly{9,9-bis[*N*,*N*-(trimethylammonium)hexyl] fluorene-*co*-1,4-phenylene} halides with average chain lengths of ~6, 12, and 100 repeat units (PFP-NR3$_{6(I),12(Br),100(Br)}$), in acetonitrile/water (see Figure 1).

## 2. EXPERIMENTAL SECTION

**2.1. Materials.** Three different poly {9,9-bis[*N*,*N*-(trimethylammonium)hexyl] fluorene-*co*-1,4-phenylene} halides, having approximately 6 (PFP-NR3$_{6(I)}$), 12 (PFP-NR3$_{12(Br)}$), and 100 (PFP-NR3$_{100(Br)}$) repeat units, were used. PFP-NR3$_{6(I)}$ was a gift from Professor Ullrich Scherf (Bergische Universität, Wuppertal) and PFP-NR3$_{12(Br)}$ and PFP-NR3$_{100(Br)}$ were gifts from Dr. Ricardo Mallavia (Universidad Miguel Hernández). PFP-NR3$_{6(I)}$ contains iodide counterions, whereas the PFP-NR3$_{12(Br)}$ and PFP-NR3$_{100(Br)}$ polymers contain bromide counterions. All were used as received. Their synthesis and characterization have been reported elsewhere.[39,40] All other chemicals were purchased from Sigma-Aldrich. Acetonitrile and ethanol were of spectroscopic grade, and Millipore Milli-Q deionized water was used throughout.

**2.2. Equipment and Methods.** *Aggregation Studies.* A $5.2 \times 10^{-5}$ M (in terms of the repeat unit of the polymer) stock solution of PFP-NR3 was prepared in water and stirred for 24 h. Aliquots (200 $\mu$L) of this stock solution were then added to 5 mL volumetric flasks using a micropipet and made up to 5 mL with 1, 5, 10, 15, 20, 25, or 30% acetonitrile/water (v/v). (The 200 $\mu$L aliquots of the stock solution were also weighed to ensure that the weights were within ±0.0001 g). Absorption measurements were made using a Shimadzu UV-2100 spectrophotometer, and steady-state luminescence studies were carried out using a Jobin Yvon-Spex Fluorolog 3-22 spectrometer. Excitation and emission slits were 4.0 nm. Fluorescence spectra were corrected for the spectral response of the light source and detector.

*Anisotropy Studies.* Fluorescence anisotropies were measured for PFP-NR3$_{6(I)}$ in 25:75 acetonitrile/water (v/v) across the PFP-NR3$_{6(I)}$ concentration range of $2.15 \times 10^{-6}$ to $2.15 \times 10^{-5}$ M (in terms of repeat units). Anisotropy values are those from the emission weighted averages across the emission band, that is, from the integrated emission curves. Steady-state fluorescence anisotropy experiments were carried out using a Jobin-Yvon Fluoromax-3 spectrometer with right angle geometry and excitation and emission slits of 5.0 nm.

*Modeling Studies.* The program used to model energy-transfer kinetics, ProgClusters, has been previously used to model energy transfer between nearest-neighbor $Ln^{3+}$ pairs within a silicate structure, AV-20.[41] However, it is not specific to this system and may be applied to any system involving energy transfer in one, two dimensions (1D, 2D) or mixed 1−2D. The program sets up an array of linear repeat units interspersed with inert end group units in a statistical (random) manner, such that the distribution of repeat unit chain lengths corresponds to the experimental polymer number average molar mass with statistical (random) polymerization. Link or trap units are then introduced between polymer chains. A link unit links polymer chains together and allows for excitation migration between chains, and a trap unit quenches excitation energy. They are distributed statistically (randomly) according to probabilities entered by the programmer. It is assumed that all repeat units have an equal chance of excitation. Every repeat unit is initially excited, and the total energy remaining after each "step" of a series of energy-transfer processes is calculated. In each "step", a specified fraction of the energy remaining at each repeat unit is transferred to adjacent units, links, and traps. Energy entering a trap is lost from the array. Superimposed on this loss by trapping is an exponential decay corresponding to a presumed exponential decay of the excited repeat unit when isolated from any traps. We have typically studied arrays containing 500 000 repeat units over a series of 200 000 energy-transfer steps during each one of which 25% of the energy in a repeat unit is transferred to any adjacent repeat unit, link, or trap.

## 3. RESULTS AND DISCUSSION

**3.1. Aggregation of PFP-NR3 Polymers, Steady-State Absorption, and Fluorescence.** Considerable research has been carried out on CCP−surfactant interactions and the breaking of CCP aggregates using nonionic surfactants.[3,10,26−28] The use of nonionic surfactants has previously been reported to increase the photoluminescence of a CCP similar to PFP-NR3$_{6(I)}$ by a factor of 8, from a quantum yield of 0.03 in pure water to a quantum yield of 0.23 in the presence of $1 \times 10^{-5}$ M surfactant.[11] Organic cosolvents are also known to break up conjugated polyelectrolyte aggregates.[42,43] In our preliminary studies with acetonitrile and ethanol as cosolvents, it was found that the use of acetonitrile gave a higher fluorescence quantum yield than did ethanol; acetonitrile was, therefore, used as a cosolvent in all subsequent experiments. The change in the absorption and emission of PFP-NR3$_{6(I)}$ at various acetonitrile concentrations is shown in Figure 2.

All the PFP-NR3 polymers studied here show broad absorption and emission bands (Figure 2) with maxima in the 375 and 420 nm regions, respectively, in 25% acetonitrile. Both the absorption ($\varepsilon_{max}$) and the emission intensity ($\Phi_f$) increase with acetonitrile percentage until 25%; after this, they essentially

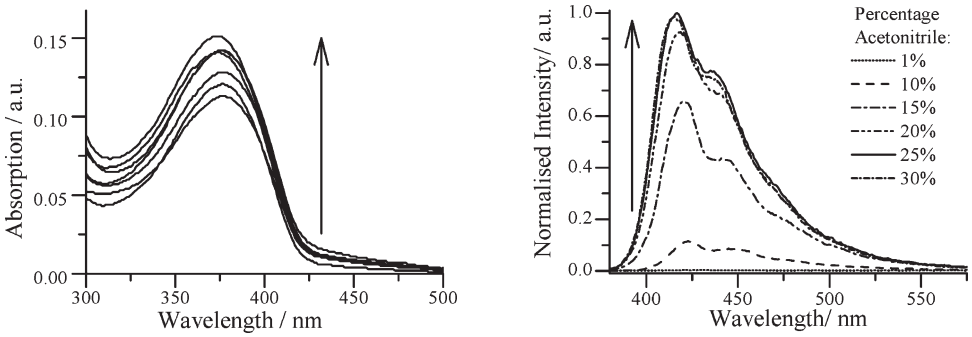


**Figure 2.** Variation in absorption (left) and emission spectra (right) of PFP-NR3$_{6(I)}$ with acetonitrile concentration (1, 10, 15, 20, 25, 30% acetonitrile in water). The direction of the arrows indicates increasing acetonitrile concentration.

**Table 1. General Photophysical Characteristics of PFP-NR3 Polymers in 25:75 Acetonitrile/Water**

| polymer | $\lambda_{max}$/nm | $\varepsilon_{max}$[a]/$10^4$ M$^{-1}$ cm$^{-1}$ | $\lambda_{emax}$/nm | $(\Phi_f)$[b] |
|---|---|---|---|---|
| PFP-NR3$_{6(I)}$ | 375 | 3.7 | 416 | 0.28 |
| PFP-NR3$_{12(Br)}$ | 375 | 3.8 | 414 | 0.34 |
| PFP-NR3$_{100(Br)}$ | 382 | 4.2 | 410 | 0.36 |

[a] $\varepsilon$ values (in terms of repeat units) are precise to $\pm 0.5 \times 10^4$ M$^{-1}$ cm$^{-1}$. [b] The error in the quantum yields is ±5%.

remain constant, before decreasing at the highest acetonitrile concentrations. The increase in $\Phi_f$ and increase in $\varepsilon_{max}$ is attributed to the breakup of polymer aggregates, although it is thought that all the PFP-NR3 polymers studied may still be aggregated to some extent even in 25:75 acetonitrile/water. It is interesting to note that PFP-NR3$_{12(Br)}$ has a much higher quantum yield (~100 times higher) in 1:99 acetonitrile/water when compared with the other PFP-NR3 polymers. With PFP-NR3$_{100(Br)}$, this may be a consequence of enhanced aggregation due to decreased solubility because of a high molecular weight, whereas with the low molecular weight PFP-NR3$_{6(I)}$, this may be attributed to it having an iodide counterion compared with the bromide counterion of PFP-NR3$_{12(Br)}$. It has previously been noted that quaternary alkylammonium salts have a higher solubility with bromide counterions as opposed to iodide counterions.[44] It is also well known that the Krafft point is higher for surfactants carrying $I^-$ counterions than $Br^-$ containing amphiphiles.[45] In addition, iodide is known to be a stronger fluorescence quencher than bromide,[46] and part of the decrease may result from counterion quenching of the PFP-NR3 emission. Work in progress is analyzing the quenching of the fluorescence of a variety of cationic conjugated polyelectrolytes by counterions. The increase in absorption and emission with acetonitrile concentration is accompanied by a slight hypsochromic wavelength shift; that is, the more aggregated polymer systems lead to longer wavelengths of maximum absorption. The fluorescence quantum yield of PFP-NR3$_{6(I)}$ in 25:75 acetonitrile/water is 0.28 (±0.01), close to, but slightly higher than, the value of 0.23 reported for the same polymer deaggregated by surfactants.[10] The absorption and emission characteristics of the PFP-NR3 polymers are given in Table 1. $\Phi_f$ and $\varepsilon_{max}$ (in terms of repeat units) increase with increasing chain length. The fluorescence of the PFP-NR3 polymers is expected to increase with the conjugation until the maximum conjugation, in agreement with the fact that PFP-NR3$_{100(Br)}$ has a higher $\Phi_f$

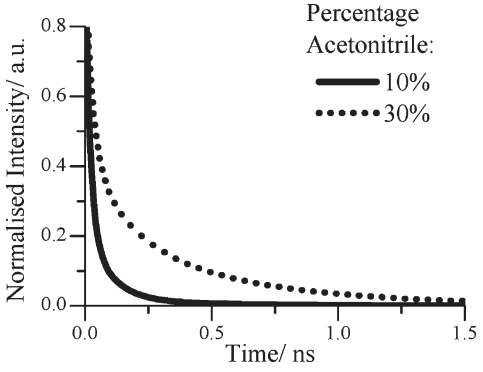


**Figure 3.** Normalized decay curves for PFP-NR3$_{6(I)}$ in 10:90 (solid line) and 30:70 (dotted line) acetonitrile/water mixtures.

**Table 2. Time-Resolved Data for PFP-NR3$_{6(I)}$ in Different Acetonitrile/Water Mixtures**

| % acetonitrile | $\alpha_1$ | $\tau_1$/ps | $\alpha_2$ | $\tau_2$/ps | $\alpha_3$ | $\tau_3$/ps |
|---|---|---|---|---|---|---|
| 10 | 0.77 | 19 | 0.22 | 93 | 0.02 | 459 |
| 15 | 0.66 | 26 | 0.29 | 103 | 0.05 | 524 |
| 20 | 0.61 | 27 | 0.24 | 124 | 0.15 | 539 |
| 25 | 0.56 | 27 | 0.23 | 142 | 0.21 | 539 |
| 30 | 0.55 | 27 | 0.23 | 153 | 0.22 | 536 |

than PFP-NR3$_{6(I)}$. However, the increase in $\Phi_f$ is not proportional to the increase in chain length as defects and twists in the polymer chains limit the conjugation, and it is likely that saturation occurs between PFP-NR3$_{12(Br)}$ and PFP-NR3$_{100(Br)}$. Also, there is a relatively large increase in $\Phi_f$ between PFP-NR3$_{6(I)}$ and PFP-NR3$_{12(Br)}$; this can be attributed to both the increase in chain length and, as already discussed, the fact that PFP-NR3$_{12(Br)}$ contains bromide counterions, which results in both a higher solubility and less efficient counterion quenching, when compared with PFP-NR3$_{6(I)}$. As can be seen in Table 1, increasing the chain length of the PFP-NR3 polymers gives a decrease in the Stokes shift. It is not immediately obvious why this should be the case, but the Stokes shifts may be affected by aggregation, specific solvation in the 25% acetonitrile/water solution, and/or energy transfer.

**3.2. Picosecond Time-Resolved Emission.** Figure 3, which shows emission decay curves for PFP-NR3$_{6(I)}$ in 10% and 30% acetonitrile/water mixtures, is representative of all the PFP-NR3

**Table 3. Time-Resolved Average Lifetime Data for the PFP-NR3 Polymers in Different Acetonitrile/Water Mixtures**

| % acetonitrile | PFP-NR3$_{6(I)}$ $\langle\tau\rangle$/ps | PFP-NR3$_{12(Br)}$ $\langle\tau\rangle$/ps | PFP-NR3$_{100(Br)}$ $\langle\tau\rangle$/ps |
|---|---|---|---|
| 10 | 134 | 461 | 52 |
| 15 | 245 | 420 | 124 |
| 20 | 377 | 423 | 213 |
| 25 | 410 | 454 | 283 |
| 30 | 410 | 459 | 306 |

decay curves. In all cases, analysis using a sum of exponentials required three decay functions to obtain a good fit to the measured data ($\chi \approx 1$). Table 2 collects kinetic data from analysis using eq 1

$$I(t) = \sum_{i=1}^{i=3} a_i \exp(-t/\tau_i) \quad (1)$$

where $a_i$ represent the amplitudes of component $i$ at $t = 0$ and $\tau_i$ the corresponding decay time. Fractional contributions were calculated from eq 2

$$f_i = \frac{a_i\tau_i}{\sum_{i=1}^{i=3} a_i\tau_i} \quad (2)$$

where $a_i\tau_i$ is the area under the decay curve for each decay component. The fractional density of each component was obtained using eq 3:

$$\alpha_i = \frac{a_i}{\sum_{i=1}^{i=3} a_i} \quad (3)$$

For all three polymers, lifetimes for the fast (~30 ps) and slow decays (~500 ps) are reasonably constant across all solvent mixtures between 15:85 and 30:70 acetonitrile/water, whereas that of the middle lifetime component decreases significantly with decreasing acetonitrile content and hence increasing aggregation (Table 2). Furthermore, the fractional contribution of the longest lifetime, which we assume to be emission from single chains of polymer,[15] increases significantly for all PFP-NR3 polymers studied with increasing acetonitrile concentration. Table 2 shows time-resolved data for PFP-NR3$_{6(I)}$ in different acetonitrile/water mixtures as an example; the time-resolved data for the longer-chain PFP-NR3's studied are available in the Supporting Information. It is suggested that the intermediate lifetime is associated with aggregated species and clusters, and thus, this would suggest that, even at optimum cosolvent concentrations, there is some aggregation.[16] The fastest component has also been suggested to indicate aggregate formation.[16] However, we note from studies on polyfluorenes[47] that the fastest component is also likely to have a major contribution from conformational relaxation on the fluorene−phenylene backbone, which is likely to be affected by the degree of aggregation. Although, in 25% acetonitrile, the fractional contributions of the short and intermediate lifetimes are high, ca. 0.79 for PFP-NR3$_{6(I)}$, relatively high $\Phi_f$ values are obtained because the long lifetime, single-chain, component makes the major contribution to the steady-state intensity.

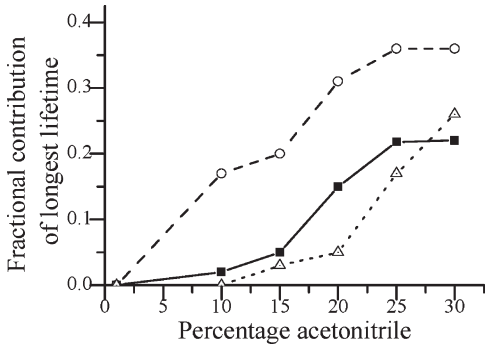


**Figure 4.** Fractional contribution of the longest lifetime of PFP-NR3$_{6(I)}$ (solid line, solid squares), PFP-NR3$_{12(Br)}$ (dashed line, open circles), and PFP-NR3$_{100(Br)}$ (dotted line, open triangles) with increasing acetonitrile concentration.

The decrease in aggregation with increasing cosolvent is also highlighted by an increase in the average lifetime for PFP-NR3$_{6(I)}$ and PFP-NR3$_{100(Br)}$, which is, in essence, a reflection of the steady-state intensity (Table 3). The average fluorescence lifetime, $\langle\tau\rangle$, can be estimated using eq 4

$$\langle\tau\rangle = \frac{\sum a_i\tau_i^2}{\sum a_i\tau_i} \quad (4)$$

The average lifetime for PFP-NR3$_{12(Br)}$ does not change a great deal with acetonitrile/water ratio. This may be a balance between PFP-NR3$_{12(Br)}$ having a higher solubility than the other two PFP-NR3 polymers and differences in the intrachain exciton migration and emission compared with deactivation at trap sites.

Figure 4 shows the change in the fractional contribution of the longest lifetime with increasing acetonitrile concentration. We assume that this reflects an increase in the concentration of isolated chains in solution with increasing acetonitrile concentration. The increase in the contribution of the longest lifetime component at 30% acetonitrile−water with PFP-NR3$_{100(Br)}$ compared with the other two PFP-NR3's probably shows that more cosolvent is needed to break up the aggregates of this higher molecular weight polymer. This is supported by the observation that, at all concentrations, the lifetime of the longest component of PFP-NR3$_{100(Br)}$ is still shorter than that of the other two PFP-NR3's. Figure 4 also further highlights the fact that PFP-NR3$_{12(Br)}$ has a higher solubility that the other two PFP-NR3s, due to a relatively short chain length and the presence of bromide counterions.

Figure 5 compares quantum yields from steady-state measurements with those calculated from normalized emission decay curves for PFP-NR3$_{6(I)}$. These data show that the decrease in quantum yield with decreasing percent acetonitrile is not due to static quenching; that is, there are no other additional decay components occurring faster than the time resolution of the instrument.

**3.3. Modeling PFP-NR3 Aggregation and Energy Transfer.** We use a model in which energy transfer from monomer to monomer, and monomer to aggregate trap, is a random walk. Energy transfer occurs in 1D, along the linear polymer chains, while energy is trapped, and lost, at aggregate trap sites that link polymer chains.

The array of repeat units, end groups, and links required to model energy transfer in a polymer was set up as follows. First, an array of 50 lines of 200 000 units of polymer repeat units and end

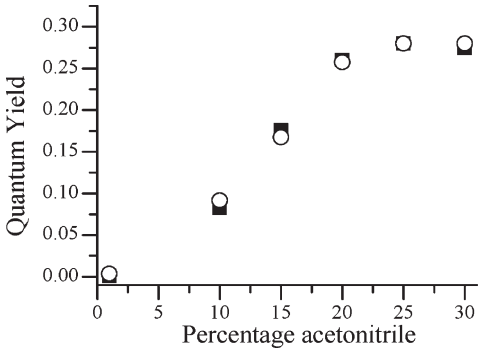


**Figure 5.** Comparison of quantum yield changes as a function of acetonitrile concentration from steady-state (solid squares) and normalized time-resolved emission decay curves (open circles) for PFP-NR3$_{6(I)}$ normalized to the measured yield of 0.28 at 25% acetonitrile.

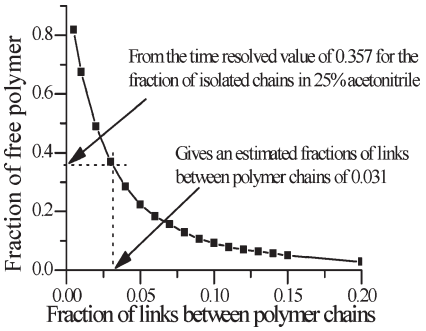


**Figure 6.** Calibration graph created using ProgClusters giving the correlation between the fraction of polymer repeat units in isolated chains and the link trap-to-repeat unit ratio.

groups was created using a random distribution of end groups and polymer repeat units at the required ratio to match the experimentally determined polymer molecular weight (e.g., 1:100 for PFP-NR3$_{100(Br)}$). This gives an array of isolated polymer chains with the same chain length distribution as would be generated by random polymerization. At this stage, there are no aggregate trap sites linking chains, and thus, the only excited-state decay routes possible are those found in isolated polymer chains. Under these circumstances, the excited-state repeat units in all of the polymer chains would be expected to decay with essentially the same first-order kinetics, with a rate constant something like the long decay time found in the multiexponential analysis of the polymer decay kinetics.

The ratio of the number of randomly placed link traps between polymer chains to the number of polymer repeat units was then calculated from a calibration graph obtained by running ProgClusters with different ratios of link traps to repeat units for each polymer and noting the fraction of isolated polymer repeat units (i.e., a repeat unit not in contact by energy migration with any aggregate trap) that remained at the end of the simulation. This produced the calibration graph, Figure 6. The fraction of repeat units in isolated chains in the polymer solution was estimated from the fraction of the long component in the time-resolved data. This value, combined with the calibration graph described above, was used to estimate the ratio of link traps to repeat units for the polymer solution; these are given for PFP-NR3$_{12(Br)}$ in different acetonitrile/water solvent mixtures in Table 4.

The fluorescence decay curve was then simulated on the array of repeat units end groups and link traps using a first-order unquenched decay rate constant superimposed on an energy-transfer random walk from excited-state repeat units into link traps in which any energy transferred into a link trap is lost from the array. Once the array is set, the simulation thus has two variables: the energy-transfer rate constant and the unquenched decay rate constant. These were varied over a range of increments and the resulting simulation compared to the experimental data (Figure 7). We could not run a rigorous statistical analysis to obtain the best-fit parameters, but we estimate, from the sensitivity of the decay curve to variation in the two parameters, that our comparison by eye gave best-fit values that we estimate are within ~20% of those we might expect from a statistical optimization. The fit from the model is in good agreement with the experimental data and is capable of generating the general curve shape and the general kinetic features associated with

**Table 4. Estimated Ratio of Link Traps to Repeat Units for PFP-NR3$_{12(Br)}$ Polymer Chains As Calculated Using ProgClusters**

| % acetonitrile | fraction of repeat units in isolated chains from time-resolved data | estimated ratio of link traps to repeat units |
|---|---|---|
| 10 | 0.174 | 0.063 |
| 15 | 0.195 | 0.057 |
| 20 | 0.312 | 0.037 |
| 25 | 0.357 | 0.031 |

aggregation. For PFP-NR3$_{12(Br)}$, the modeled rate constant for unquenched decay is $1.9 \times 10^9$ s$^{-1}$ and the rate constant for energy transfer, both between repeat units and from repeat units to traps, is $2.4 \times 10^{12}$ s$^{-1}$. For PFP-NR3$_{100(Br)}$, these values are $2.0 \times 10^9$ s$^{-1}$ and $5.2 \times 10^{12}$ s$^{-1}$, respectively (these modeled rate constants, generated from ProgClusters, will be identified by the subscript PC).

We can compare these rate constants from the model fits to experimental and/or theoretical values. The best-fit model rate constant for unquenched decay is very similar to that for the long-lived lifetime found in the multiexponential fit of time-resolved data, whereas the energy-transfer rate constant can be compared to the calculated value for FRET. Table 5 collects FRET data for all PFP-NR3 polymers. The calculated rate constant for PFP-NR3$_{6(I)}$ for energy transfer, $k_{ET}$, from repeat unit to repeat unit is $3.9 \times 10^{12}$ s$^{-1}$. The calculated Förster distance, the distance at which the energy-transfer rate is equal to that of unquenched decay, is 2.78 nm, in good agreement with a reported value for a related fluorene−phenylene polymer, PFP, of 2.95 nm.[36] These values highlight the extremely fast energy transfer possible along and between polymer chains. The increase in the calculated FRET rate constant with polymer chain length shown in Table 5 is due to corresponding increases in $\varepsilon_{max}$ with chain length; it is interesting to note a similar increase in energy-transfer rate constants with increasing chain length for values obtained from the curve fit of ProgClusters.

We note that $k_{PC}$ is slightly lower than $k_{ET}$, possibly because energy transfer into an aggregate trap is slower than from repeat unit to repeat unit.

**3.4. Fluorescence Anisotropy of PFP-NR3$_{6(I)}$.** To confirm the existence of aggregation in these systems, we have studied the

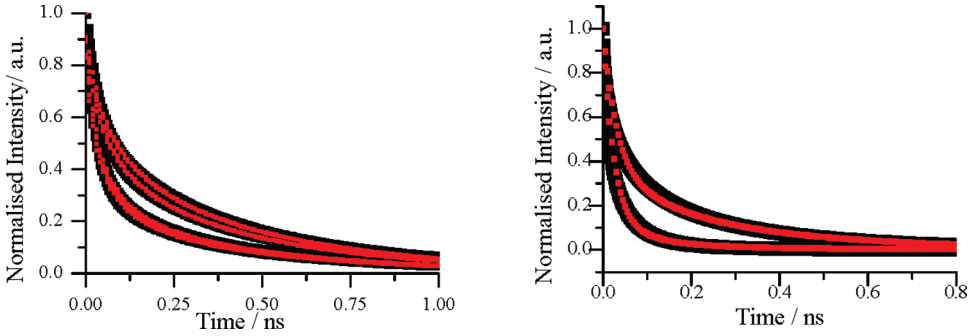


**Figure 7.** Time-resolved decays curves for PFP-NR3$_{12(Br)}$ with 10, 15, 20, and 25% acetonitrile (left, black) and PFP-NR3$_{100(Br)}$ with 1% and 25% acetonitrile (right, black) and modeled decay curves (red).

**Table 5. Förster Distance, Calculated FRET Rate Constants for Repeat Unit-to-Repeat Unit Energy Transfer, $k_{ET}$, and Rate Constants for Repeat Unit-to-Repeat Unit Energy Transfer from ProgClusters, $k_{PC}$**

| polymer | Förster distance/nm | $k_{ET}/s^{-1}$ | $k_{PC}/s^{-1}$ |
|---|---|---|---|
| PFP-NR3$_{6(I)}$ | 2.78 | $3.9 \times 10^{12}$ | |
| PFP-NR3$_{12(Br)}$ | 3.01 | $6.2 \times 10^{12}$ | $2.4 \times 10^{12}$ |
| PFP-NR3$_{100(Br)}$ | 3.08 | $7.3 \times 10^{12}$ | $5.2 \times 10^{12}$ |

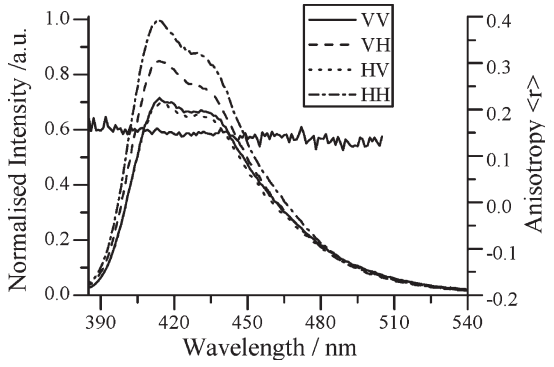


**Figure 8.** Normalized polarized emission of PFP-NR3$_{6(I)}$ in acetonitrile/water (25:75 v/v). The inset in the figure gives the alignment of the polarizers for the relevant spectrum. The anisotropy value is shown by the solid line across the band.

behavior of PFP-NR3$_{6(I)}$ as a function of concentration in 25% acetonitrile−water using fluorescence anisotropy. The steady-state polarized spectra for PFP-NR3$_{6(I)}$ in a solution of 25:75 acetonitrile/water (v/v) is shown in Figure 8. The anisotropy varies little across the emission band, with an average anisotropy of 0.14 which can be compared with theoretical values of 0.4 for zero depolarization and 0 for full depolarization.

It was found that the fluorescence anisotropy decreased with increasing PFP-NR3$_{6(I)}$ concentration (Figure 9). We interpret this depolarization as due to resonance energy transfer both along and between polymer chains, because increasing the concentration of PFP-NR3$_{6(I)}$ increases aggregation and thus facilitates interchain energy transfer.

The anisotropy of PFP-NR3$_{6(I)}$ was also measured in various acetonitrile/water mixtures. As expected, the anisotropy of PFP-NR3$_{6(I)}$ decreases substantially with a decrease in the percentage

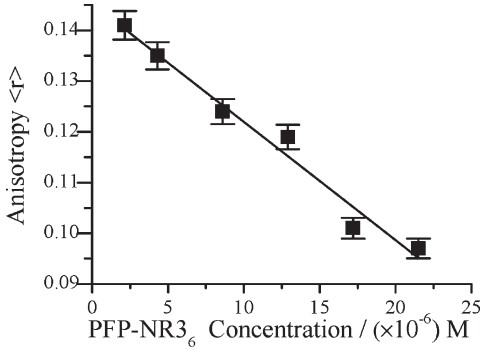


**Figure 9.** Average anisotropy as a function of PFP-NR3$_{6(I)}$ concentration.

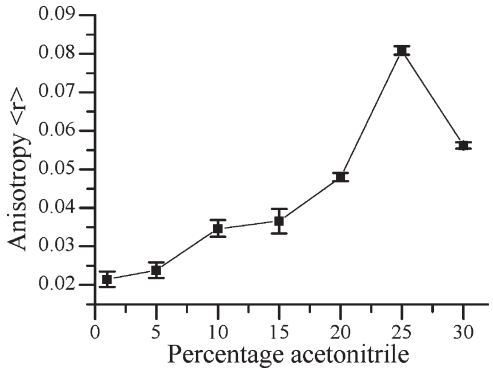


**Figure 10.** Change in anisotropy of PFP-NR3$_{6(I)}$ with various fractions of the cosolvent acetonitrile in acetonitrile/water mixtures.

of acetonitrile (Figure 10), again presumably due to interchain energy transfer as a consequence of increased aggregation.

The anisotropy results also support the previous conclusion that 25% acetonitrile as a cosolvent is optimum for decreasing aggregation. The change in anisotropy with solvent composition not only highlights the effect of the cosolvent on the degree of aggregation but also supports the idea that interchain energy transfer is the dominant mechanism for depolarization because an increase in aggregation significantly increases the probability of neighboring monomers being close enough for FRET. In the case of FRET between chemically identical molecules, fluorescence anisotropy can be resolved into two terms: depolarization by molecular rotation and depolarization by energy transfer.[48] In the case of these polymers, depolarization is believed to be due

only to energy transfer, as the polymer is essentially static over the fluorescence lifetime.[43]

## 4. CONCLUSIONS

Addition of acetonitrile as a cosolvent breaks up aggregates of PFP-NR3 formed in water. This is reflected by an ~10-fold increase in fluorescence quantum yield, a ca. 2-fold increase in the molar extinction coefficient, an increase in the fractional contribution to the lifetime of isolated chains in time-resolved measurements, and an ~4 fold increase in the fluorescence anisotropy. However, even at optimum acetonitrile/water mixtures of ca. 25:75, there may still be some aggregation. If the two shorter lifetimes of the PFP-NR3 polymers from time-resolved analysis are associated with aggregated species or clusters, this would confirm that, even at optimum cosolvent concentrations, there is a degree of aggregation. Steady-state fluorescence anisotropy of PFP-NR3$_{6(I)}$ decreases with increasing aggregation. This decrease in anisotropy is attributed to increased fluorescence depolarization by interchain energy transfer in aggregated PFP-NR3$_{6(I)}$. Energy migration along the PFP-NR3 chains is probably via a FRET mechanism because the calculated rate constants for energy transfer from repeat unit to repeat unit are very high ($\approx 10^{12}$–$10^{13}$ s$^{-1}$) and the repeat unit separation of 0.840 nm is very much shorter than the Förster distance of ca. 3 nm. The time-resolved emission decay curves for PFP-NR3$_{12(Br)}$ and PFP-NR3$_{100(Br)}$ in different acetonitrile/water mixtures, and thus different degrees of aggregation, have been successfully modeled in terms of a series of energy-transfer steps where energy is quenched at an aggregate trap where two polymer chains meet. These modeling studies give rate constants of $\approx 2 \times 10^9$ s$^{-1}$ for the natural decay of an isolated repeat unit and $2.4 \times 10^{12}$ and $5.2 \times 10^{12}$ s$^{-1}$ for energy transfer in PFP-NR3$_{12(Br)}$ and PFP-NR3$_{100(Br)}$, respectively. These values are in good agreement with (a) the longest decay rate constant obtained by picosecond emission studies and (b) those calculated for FRET, $6.2 \times 10^{12}$ and $7.3 \times 10^{12}$ s$^{-1}$ for PFP-NR3$_{12(Br)}$ and PFP-NR3$_{100(Br)}$, respectively.

Two of the polymers (PFP-NR3$_{12(Br)}$ and PFP-NR3$_{100(Br)}$) have bromide counterions, whereas the third (PFP-NR3$_{6(I)}$) is the iodide salt. Although we do not believe that this has any significant effect on the aggregation at the polymer concentrations studied, there are indications of fluorescence quenching by counterions in these systems. A future publication will present a detailed study of the effect of counterions on the photophysics of cationic conjugated polyelectrolytes.

All PFP-NR3 polymers studied have high fluorescence quantum yields and molar extinction coefficients in optimum acetonitrile/water mixtures, properties that are advantageous for the use of the PFPs in optoelectronics or materials applications. The chemical structure of these PFP-NR3 polymers may be useful as the responsive basis for biological and chemical detection designs based on optical properties because it allows for effective electronic coupling and fast intra- and interchain energy transfer; thus, the polymer chain can act as a path for the transfer of excitation energy to energy acceptors and quenchers.

## ■ ASSOCIATED CONTENT

**Ⓢ Supporting Information.** Changes in emission with solvent cofraction for PFP-NR3$_{12(Br)}$ and PFP-NR3$_{100(Br)}$ are given. Full tables of picosecond fluorescence lifetime data are available. Typical ProgClusters arrays that show the loss of excitation energy with increasing number of energy-transfer steps for PFP-NR3$_{12(Br)}$ are given as a representative example of the model scheme. The calculation of FRET rates and degree of spectral overlap of the PFP-NR3's is discussed. This material is available free of charge via the Internet at http://pubs.acs.org.

## ■ AUTHOR INFORMATION

### Corresponding Author

*Phone: +44 (0)1248 382375 (M.L.D.), +44 (0)1792 513081 (P.D.), +351 239854482 (H.D.B.). E-mail: m.davies@bangor.ac.uk (M.L.D.), P.Douglas@swansea.ac.uk (P.D.), burrows@ci.uc.pt (H.D.B.).

### Present Addresses

⊥The School of Chemistry, Bangor University, Bangor, Gwynedd, LL57 2UW, U.K.

## ■ ACKNOWLEDGMENT

This work was supported by a grant from an EU Research Training Network, CIPSNAC (Colloidal and Interfacial Properties of Synthetic Nucleic Acid Complexes, Contract No. MRTN-CT-2003-504932). We thank Professor U. Scherf and Dr Ricardo Mallavia for the kind gift of the conjugated polyelectrolytes (PFP-NR3's), NEONUCLEI and Swansea University for financial support, and POCI/FCT/FEDER for further financial support through the Projects POCTI/QUI/45344/2002, POCI/QUI/58291/2004, POCTI/QUI/58689/2004, and PTDC/QUI/67962/2006. We are grateful to Prof Sergio Seixas de Melo, Dr. J. Pina, and Dr. F. Dias for access to, and help with, TCSPC equipment at the Chemistry Laser Lab Coimbra (CLLC).

## ■ REFERENCES

(1) Davies, M. L.; Burrows, H. D.; Morán, M. C.; Miguel, M. G.; Douglas, P. *Biomacromolecules* **2009**, *10*, 2987.

(2) Liu, B.; Bazan, G. C. *Chem. Mater.* **2004**, *16*, 4467.

(3) (a) Burrows, H. D.; Lobo, V. M. M.; Pina, J.; Ramos, M. L.; Seixas de Melo, J.; Valente, A. J. M.; Tapia, M. J.; Pradhan, S.; Scherf, U. *Macromolecules* **2004**, *37*, 7425. (b) Burrows, H. D.; Tapia, M. J.; Fonseca, S. M.; Pradhan, S.; Scherf, U.; Silva, C. L.; Pais, A. A. C. C.; Valente, A. J. M.; Schillén, K.; Alfredsson, V.; Carnerup, A. M.; Tomsic, M.; Jamnik, A. *Langmuir* **2009**, *25*, 5545.

(4) Gaylord, B. S.; Heeger, A. J.; Bazan, G. C. *J. Am. Chem. Soc.* **2003**, *125*, 896.

(5) Wang, S.; Liu, B.; Gaylord, B. S.; Bazan, G. C. *Adv. Funct. Mater.* **2003**, *13*, 463.

(6) Gaylord, B. S.; Wang, S.; Heeger, A. J.; Bazan, G. C. *J. Am. Chem. Soc.* **2001**, *123*, 6417.

(7) (a) Pinto, M. R.; Schanze, K. S. *Synthesis* **2002**, *9*, 1293. (b) Jiang, H.; Taranekar, P.; Reynolds, J. R.; Schanze, K. S. *Angew. Chem., Int. Ed.* **2009**, *48*, 4300.

(8) Hoven, C. V.; Garcia, A.; Bazan, G. C.; Nguyen, T. Q. *Adv. Mater.* **2008**, *20*, 3793.

(9) Wågberg, T.; Liu, B.; Orädd, G.; Eliasson, B.; Edman, L. *Eur. Polym. J.* **2009**, *45*, 3230.

(10) Al Attar, H. A.; Monkman, A. P. *J. Phys. Chem. B* **2007**, *111*, 12418.

(11) Leclerc, M. *Adv. Mater.* **1999**, *11*, 1491.

(12) McQuade, D. T.; Pullen, A. E.; Swager, T. M. *Chem. Rev.* **2000**, *100*, 2537.

(13) Thomas, S. W.; Joly, G. D.; Swager, T. M. *Chem. Rev.* **2007**, *107*, 1339.

(14) Achyuthan, K. E.; Bergstedt, T. S.; Chen, L.; Jones, R. M.; Kumaraswamy, S.; Kushon, S. A.; Ley, K. D.; Lu, L.; McBranch, D.; Mukundan, H.; Rininsland, F.; Shi, X.; Xia, W.; Whitten, D. G. *J. Mater. Chem.* **2005**, *15*, 2648.
(15) Fan, C.; Plaxco, K. W.; Heeger, A. J. *Trends Biotechnol.* **2005**, *23*, 186.
(16) Al-Attar, H. A.; Monkman, A. P. *Adv. Funct. Mater.* **2008**, *18*, 2498.
(17) Chi, C.; Mikhailovsky, A.; Bazan, G. C. *J. Am. Chem. Soc.* **2007**, *129*, 11134.
(18) Pu, K. Y.; Pan, S. Y. H.; Liu, B. *J. Phys. Chem. B* **2008**, *112*, 9295.
(19) (a) Monteserín, M.; Burrows, H. D.; Valente, A. J. M.; Mallavia, R.; Di Paolo, R. E.; Maçanita, A. L.; Tapia, M. J. *J. Phys. Chem. B* **2009**, *113*, 1294. (b) Tapia, M. J.; Monteserín, M.; Valente, A. J. M.; Burrows, H. D.; Mallavia, R. *Adv. Colloid Interface Sci.* **2010**, *158*, 94.
(20) Anestopoulos, D.; Fakis, M.; Persephonis, P.; Giannetas, V.; Mikroyannidis, J. *Chem. Phys. Lett.* **2006**, *421*, 205.
(21) Chen, L.; McBranch, D. W.; Wang, H.; Helgeson, R.; Wudl, F.; Whitten, D. *Proc. Natl. Acad. Sci. U.S.A.* **1999**, *96*, 12287.
(22) Gaylord, B. S.; Heeger, A. J.; Bazan, G. C. *Proc. Natl. Acad. Sci. U.S.A.* **2002**, *99*, 10954.
(23) Ho, H. A.; Bera-Aberem, M.; Leclerc, M. *Chem.—Eur. J.* **2005**, *11*, 1718.
(24) Davies, M. L.; Douglas, P.; Burrows, H. D.; Miguel, M. G.; Douglas, A. *Port. Electrochim. Acta.* **2009**, *27*, 525.
(25) Wang, Y.; Erdogan, B.; Wilson, J. N.; Bunz, U. H. F. *Chem. Commun.* **2003**, 1624.
(26) Chen, L. H.; Xu, S.; McBranch, D.; Whitten, D. *J. Am. Chem. Soc.* **2000**, *122*, 9303.
(27) Lavigne, J. J.; Broughton, D. L.; Wilson, J. N.; Erdogan, B.; Bunz, U. H. F. *Macromolecules* **2003**, *36*, 7409.
(28) Burrows, H. D.; Lobo, V. M. M.; Pina, J.; Ramos, M. L.; Seixas de Melo, J.; Valente, A. J. M.; Tapia, M. J.; Pradhan, S.; Scherf, U.; Hintschich, S. I.; Rothe, C.; Monkman, A. P. *Colloids Surf., A* **2005**, *270*, 61.
(29) Chen, P.; Yang, G. Z.; Liu, T. X.; Li, T. C.; Wang, M.; Huang, W. *Polym. Int.* **2006**, *55*, 473.
(30) Bredas, J. L.; Beljonne, D.; Coropceanu, V.; Cornil, J. *Chem. Rev.* **2004**, *104*, 4971.
(31) Burrows, H. D.; Fonseca, S. M.; Silva, C. L.; Pais, A. A. C. C.; Tapia, M. J.; Pradhan, S.; Scherf, U. *Phys. Chem. Chem. Phys.* **2008**, *10*, 4420.
(32) Ruseckas, A.; Wood, P.; Samuel, I. D. W.; Webster, G. R.; Mitchell, W. J.; Burn, P. L.; Sundstrom, V. *Phys. Rev. B* **2005**, *72*, 115214.
(33) Markov, D. E.; Blom, P. W. M. *Phys. Rev. B* **2006**, *74*, 085206.
(34) Dias, F. B.; Knaapila, M.; Monkman, A. P.; Burrows., H. D. *Macromolecules* **2006**, *39*, 1598.
(35) Förster, T. *Ann. Phys.* **1948**, *437*, 55.
(36) Montilla, F.; Frutos, L. M.; Mateo, C. R.; Mallavia, R. *J. Phys. Chem. C* **2007**, *111*, 18405.
(37) Förster, T. *Discuss. Faraday Soc.* **1959**, *27*, 7.
(38) Perrin, F. *Ann. Phys.* **1932**, *17*, 283.
(39) Pradhan, S. Ph.D. Dissertation, Bergischen Universität Wuppertal, 2004.
(40) Montserín, M.; Tapia, M. J.; Ribeiro, A. C. F.; Santos, C. I. A. V.; Valente, A. J. M.; Burrows, H. D.; Mallavia, R.; Nilsson, M.; Söderman, O. *J. Chem. Eng. Data* **2010**, *55*, 1860.
(41) Evans, R. C.; Ananias, D.; Douglas, A.; Douglas, P.; Carlos, L. D.; Rocha, J. *J. Phys. Chem. C* **2008**, *112*, 260.
(42) Pina, J.; Seixas de Melo, J.; Burrows, H. D.; Maçanita, A. L.; Galbrecht, F.; Bünnagel, T.; Scherf, U. *Macromolecules* **2009**, *42*, 1710.
(43) Levitsky, I. A.; Kim, J.; Swager, T. M. *J. Am. Chem. Soc.* **1999**, *121*, 1466.
(44) Scibona, G.; Danesi, P. R.; Conte, A.; Scuppa, B. *J. Colloid Interface Sci.* **1971**, *35*, 631.
(45) Holmberg, I.; Jonsson, B.; Kronberg, B.; Lindman, B. *Surfactants and Polymers in Aqueous Solution*, 2nd ed.; Wiley: Chichester, U.K., 2003.
(46) Watkins, A. R. *J. Phys. Chem.* **1974**, *78*, 2555.
(47) Dias, F. B.; Maçanita, A. L.; Seixas de Melo, J.; Burrows, H. D.; Güntner, R.; Scherf, U.; Monkman, A. P. *J. Chem. Phys.* **2003**, *118*, 7119.
(48) Lakowicz, I. R. *Principles of Fluorescence Spectroscopy*, 3rd ed.; Plenum Press: New York, 2006.